UC Berkeley

UC Berkeley Previously Published Works

Title

Simultaneous inversion of multiple microseismic data for event locations and velocity model with Bayesian inference

Permalink

https://escholarship.org/uc/item/1vs2s1vs

Authors

Zhang, Z
Rector, JW
Nava, MJ

Publication Date

2016

DOI

10.1190/segam2016-13850020.1

Peer reviewed

eScholarship.org Powered by the California Digital Library
University of California

Simultaneous inversion of multiple microseismic data for event locations and velocity model with Bayesian inference

Zhishuai Zhang, James W. Rector, and Michael J. Nava, University of California, Berkeley

Summary

We applied Bayesian inference for simultaneous inversion of multiple microseismic data for event locations and velocity models. The traditional method of using a predetermined ve- locity model for event location is subject to large uncertainty if prior information of the velocity model is poor. Our study shows that microseismic data can improve the velocity model, which is usually a major source of location uncertainty. Also, the developed method can quantify the uncertainty of the mi- croseismic location estimation. Its successful application on both synthetic examples and Newberry enhanced geothermal system (EGS) demonstrates its robustness over the traditional least-square traveltime inversion. Comparison with location result of the traditional method shows that we can effectively improve the accuracy of microseismic event location thanks to the improved velocity model.

Introduction

Traditional methods for microseismic event location include least-square traveltime inversion (Aki and Richards, 1980), co- herence scanning (Drew et al., 2005; Duncan Peter and Eisner, 2010), double-difference (Waldhauser and Ellsworth, 2000), etc. Due to the lack of information on velocity models and limited spatial coverage of monitoring stations, microseismic location uncertainty can be significant (Eisner et al., 2009; Maxwell, 2009; Hayles et al., 2011; Warpinski et al., 2009). As such, it is crucial to obtain a quantitative understanding of microseismic event location uncertainty before drawing any further conclusions on microseismic data.

Velocity information is usually obtained independently from microseismic data, such as from sonic logs, active source sur- vey, or subsurface calibration/perforation shots. However, in a realistic survey, it can be challenging to build even a one- dimensional model due to lacked or poor quality of informa- tion. On the other hand, the seismic waveform carries information on earth structure. Given the abundance of microseismic events in a normal survey, they are a good source of informa- tion to calibrate or even construct a velocity model for micro- seismic location (Douglas, 1967).

Various techniques have been developed to improve a veloc- ity model with arrival times (Zhang and Thurber, 2003; Zhang et al., 2009; Zhou et al., 2010; Li et al., 2013). Though ef- fective to a certain extent, these methods do not follow a rig- orous statistical framework. This makes the determination of various parameters, such as weighting and regularization, very challenging (Monteiller et al., 2005). Bayesian inference is a widely used algorithm in subsurface inverse problems (Oliver et al., 2008; Tarantola and Valette, 1982; Tarantola, 2005; Zhang et al., 2014). It provides a method of treating parameters as a joint probability density, it has been very successful in model parameter estimation and uncertainty analysis.

We applied the Bayesian inference for simultaneous veloc- ity inversion and event location using multiple microseismic event data. Maximum A Posteriori (MAP) estimation is used to solve for posterior probability density. The successful ap- plication of the developed method on synthetic and real micro- seismic survey demonstrates its effectiveness in simultaneous velocity inversion and event location.

Theory

The central idea of Bayesian inference is representing all the information (forward model, observation, and prior informa- tion) with probability densities and then using inversion theory to infer the posterior probability density of the model parame- ters we would like to know.

Inverse problem thoery

We can denote the model parameters and observable parame- ters (data) of a physical system as m and d, respectively. The inverse problem theory (Tarantola, 2005) gives the joint poste- rior probability density:

$$\sigma_M(m) = \rho_D(d)\rho_M(m)\theta(d|m)/\mu_D(d), \quad (1)$$

where $\rho_D(d)$ is the probability density in data space represent- ing the information given by a measurement, $\rho_M(m)$ is the prior information on model parameters, $\theta(d|m)$ is the conditional probability density of data d given model parameters m, and $\mu_D(d)$ is the homogeneous probability density in data space.

The marginal probability density of model parameters m is the integration of the joint probability density over the entire data space D:

$$\sigma_M(m) = \int_D \sigma(d, m)\, dd. \quad (2)$$

© 2016 SEG

good solution to earthquake loca- tion (Monteiller et al., 2005; Myers et al., 2007, 2009) and mi- croseismic event location problems (Poliannikov et al., 2014; Templeton et al., 2014; Zhang et al., 2015a,b). Thanks to its

spaceIf the model and data space of the system are both linear, under

Gaussian assumption, the posterior probability density of the model parameters can be expressed by

$$\sigma_M(\mathrm{m}) = c \exp[-O(\mathrm{m})], \qquad (3)$$

and

$$O(\mathrm{m}) = \frac{1}{2}[g(\mathrm{m}) - d_{obs}]^T C_D^{-1}[g(\mathrm{m}) - d_{obs}] + \frac{1}{2}(\mathrm{m} - \mathrm{m}_{prior})^T C_M^{-1}(\mathrm{m} - \mathrm{m}_{prior}), \qquad (4)$$

where $g(\cdot)$ is the forward modeler for the prediction of observ- able parameters from model parameters m. m_{prior} is the prior information on the model parameters. The covariance matrix

spaceC_D is the addition of observation uncertainty covariance ma- trix C_d and theoretical uncertainty covariance matrix C_T. C_M is the covariance matrix of the prior information uncertainty. c is a normalization constant. A derivation of equation 3 and equation 4 is presented by Tarantola (2005).

Maximum A Posteriori estimation

Both stochastic and deterministic approaches are considered in the literature for characterization of the resulting posterior probability density. Here, we use the Maximum A Posteri- ori (MAP) estimation, which aims to estimate the mode of the posterior probability density:

$$m_{MAP} = \arg\max_m \sigma_M(\mathrm{m}). \qquad (5)$$

Or frequently minimizes equation 4. It provides incomplete, yet important characterization of the conditional parameter dis- tribution.

The above minimization can be implemented using the classi- cal Gauss-Newton method. Once the MAP estimate m_{MAP} is found, the posterior covariance matrix $C_{m,MAP}$ can be approx- imated through linearization about the MAP estimate as

$$C_{m,MAP} = C_M - C_M G_{MAP}^T (G_{MAP} C_m G_{MAP}^T + C_D)^{-1} G_{MAP} C_M, \qquad (6)$$

spaceThe velocity model used for dataset construction is a multiple- layer model based on Matzel et al. (2014)'s interferometry es- timation of the velocity model at Newberry EGS site (yellow line in Figure 1). P- and S-wave travel times are calculated for each event station pair, and a Gaussian noise with standard deviation of 0.050 s is added as a representation of picking error. We assume there is little prior information on microseis- mic event locations and velocity model parameters. A mul- tivariate normal distribution with reasonable mean and suffi- ciently large standard deviation can approximate a null proba- bility density for prior information and initial model. The prior velocity model is represented by the red line in Figure 1.

The comparison between true microseismic locations and the estimated 50 % error ellipsoids is also shown in Figure 1. About half of the true locations lie in the 50 % error ellipsoids. This verifies the effectiveness of both MAP estimation and uncer- tainty approximation. We can see from Figure 1 that the true velocity model can be successfully captured by simultaneous inversion using multiple microseismic data. The MAP esti- mated velocity model is much closer to the true one compared with the prior model.

The standard deviation of the misfits between observed and modeled arrival times is 0.049 s. This is very close to 0.050 s, which is the Gaussian random noise standard deviation added to the true arrival times. This means the covariance matrix

spacewhere, G

space

MAP

spaceis the sensitivity matrix at the MAP point with

$\frac{\partial g}{\partial m}$

spaceelements $G_{ij} =$ space$_{i}$ ∂m_j

spaceMultiple-event microseismic location implementation

We include the velocity model in the model space in addition to the origin coordinates and times of all microseismic events. The velocity model used is a two-layer model with constant velocity gradient for each layer. The velocity model param- eters to be estimated include P-wave velocity at a reference depth, P-wave velocity gradient for each of the two layers, the elevation of the two layers interface, and Vp/Vs. For the prior information on model parameters, we use a homogeneous probability density since the number of observable parameters is redundant compared with model parameters. The measure- ment includes any available P- and/or S-wave arrival times for each event at each station. The forward model is for calcula- tion of arrival time from microseismic event location to seis- mic station. The ray path between two points in a constant velocity gradient layer can be obtained analytically (Slawinski and Slawinski, 1999). We solve the two-layer problem semi- analytically by iterating for the ray parameter that is common to the seismic rays in both layers.

© 2016 SEG

Synthetic example

We begin with a synthetic model as shown in Figure 1. The dataset was constructed from 30 shallow borehole stations in three lines. The stations spacing is 0.6 km in easting direc- tion and 2 km in northing direction. All the stations share a common elevation of 1.8 km. Microseismic events on three horizontal planes at the elevations of -0.5 km, -1.0 km, and
-1.5 km were assumed. The areal coverage of the stations is approximately twelve times that of the microseismic events.
spacelayer model for the simultaneous inversion problem, and the theoretical uncertainty covariance matrix C_T can be ignored in this case.

Microseismic survey in Newberry EGS demonstration

We applied the developed simultaneous inversion algorithm on a microseismic data set from Newberry EGS demonstra- tion site. Fluid injection for the hydroshearing purpose has induced microseismic events in this area. These event loca- tions have been estimated by a contractor with P- and S-wave arrival times. With the same arrival time picking information, we relocated the microseismic events with our developed al- gorithm.

Newberry EGS demonstration

The EGS system under study is located at the Newberry vol- cano in central Oregon. According to the plan (Petty et al., 2013; Osborn et al., 2010, 2011), an existing well, NGC 55-29, was stimulated with hydroshearing technique due to the high temperature and lack of permeability of the nearby formation. The well NGC 55-29 has a total depth of 3066 m with an open hole from 1790 m to its total depth. In contrast to the well- known hydraulic fracturing, the hydroshearing technique used in this demonstration stimulated the formation below its min- imum principle stress. The stimulation induced shear failures of pre-existing natural fractures in the target formation. The process was monitored with seismometers both on the surface as well as in shallow boreholes.

Microseismic survey

spaceThe survey was conducted with fifteen seismic stations, which include seven seismometers placed on the surface and eight placed in shallow boreholes as shown in Figure 2. A permitting issue leads to the poor azimuthal coverage of shallow bore- hole stations. Surface stations provide complimentary cover- age. The eight shallow monitoring holes were drilled to depths between 213 and 246 m. The primary objective is to reach be- low the water table and highly attenuating cinders and debris flows (Cladouhos et al., 2013). The stimulation of NGC 55-29 began on October 17, 2012 and concluded December 7, 2012. The first microseismic event occurred on October 29, 2012. A total of 204 events with reasonably high S/N were recorded until December 31, 2012.

To process the microseismic dataset, a contractor has picked P- and/or S-wave arrival times for all event-station pairs when- ever possible. They also derived the 1D velocity model by con- ducting dedicated active source seismic survey (red line in Fig- ure 3). With the obtained velocity model, they located the mi- croseismic events by minimizing the misfit between observed and modeled P- and/or S-wave arrival times. Figure 3 also shows the velocity model constructed by Matzel et al. (2014) with interferometry.

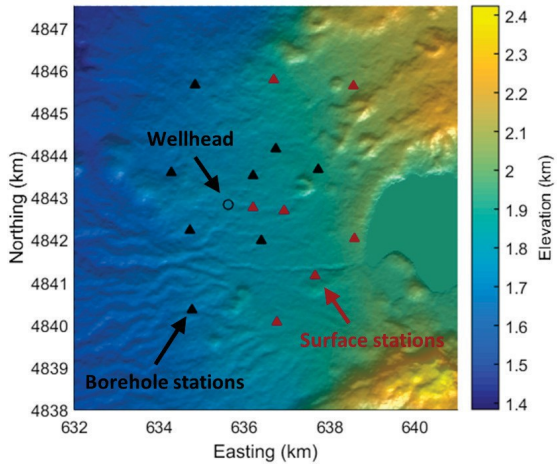

Figure 2: Map of surface stations and shallow borehole sta- tions for microseismic monitoring. Surface stations provide complimentary coverage to the shallow borehole stations.

Results and Discussion

Figure 3 shows our location result along with the result pro- cessed by the contractor. Both of the two results show two event clusters: the shallow events above 0 km elevation, and the deep events near the open hole portion of the well. The tar- get zone of the stimulaton is the formation at the depth of the open hole. However, we see much more microseismic events in the shallow area. Borehole television survey found it is a result of a fluid loss from a cracked casing. Even though these two results share a similar microseismic distribution pattern, we find the microseismic event locations provided by con- tractor (orange dots) are much more scattered than those esti- mated by our method (blue dots). The contractor's traditional method even located some events above the surface (elevation

© 2016 SEG

spaceof 1.77 km). In addition, microseismic events estimated by our method are mostly confined within or below the unit of mixed tuffs, rhyolites, and andesites which may act as a barrier to hydraulic fractures.

The right side of Figure 3 is the plot of the velocity models used by the contractor, estimated by our simultaneous inver- sion using microseismic arrival times, and obtained with seis- mic interferometry by Matzel et al. (2014). From the compar- ison, we find the velocity model estimated with our method matches the result of seismic interferometry very well. How- ever, the velocity model used by the contractor is higher than these two results at the elevation interval between 0.5 km and
1.5 km. This is the reason for the unrealistic high elevation events estimated by the contractor.

Conclusions

We built the framework for simultaneous inversion of multiple microseismic data for event locations and velocity model pa- rameters with Bayesian inference. MAP estimation gives an efficient and reasonable approximation to the posterior prob- ability distribution. Additionally, Bayesian inference enables the uncertainty to be quantified. The application of the devel- oped location algorithm on both synthetic example and New- berry EGS data successfully estimated microseismic event lo- cations and improved the velocity model. The Newberry mi- croseismic location result of the developed method is more consistent with geology information compared with that from the contractor.

Acknowledgments

We would like to thank Dr. Stephen C. Myers, Dr. Gardar Johannesson, and Dr. William Hanley at Lawrence Livermore National Laboratory for their inspiring work on Bayesloc and MicroBayesloc. We also thank Dr. Dennise Templeton at Lawrence Livermore National Laboratory for her kind help in the initial process of this work and providing access to New- berry geothermal data set.

space

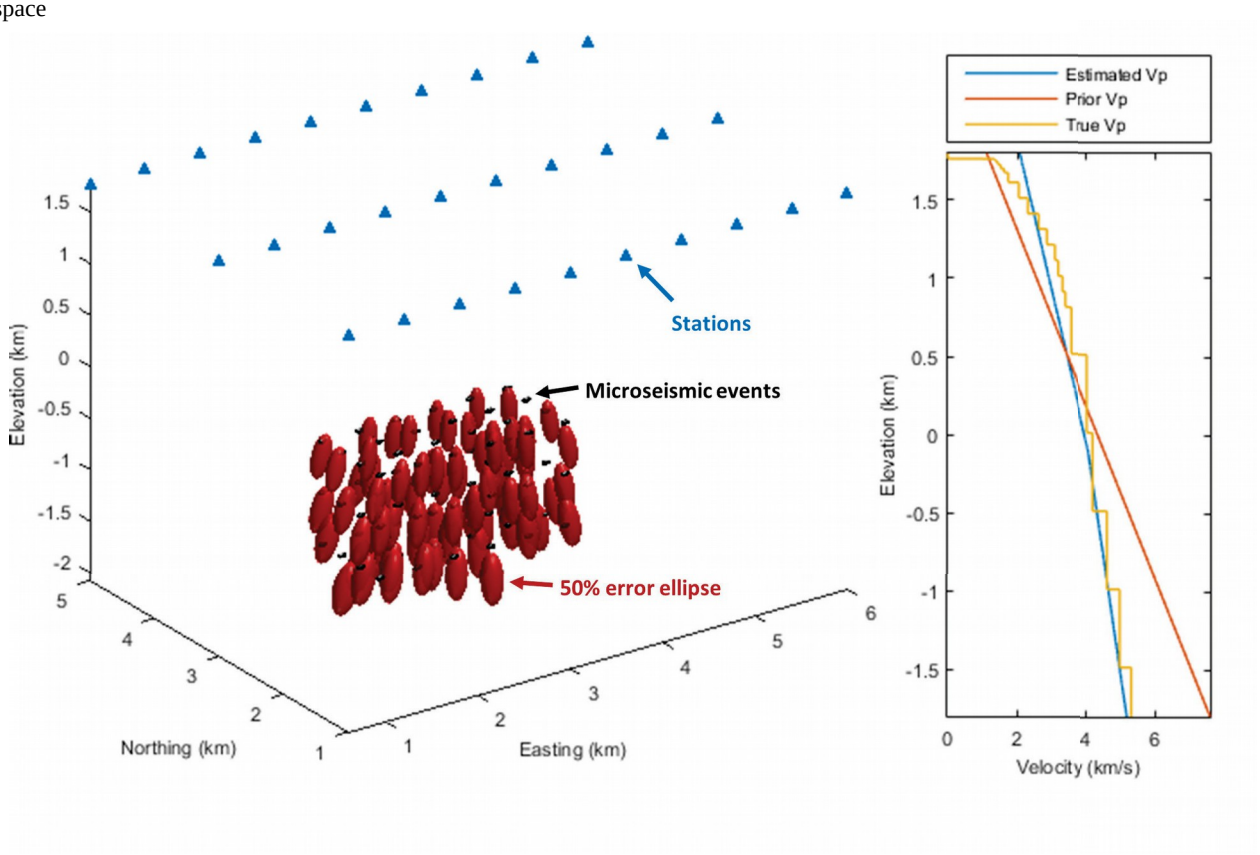

Figure 1: Synthetic example. The comparison between the true locations and estimated ones verifies the effectiveness of both MAP estimation and uncertainty approximation (left). The estimated two-layer velocity model can capture the trend of the true multiple-layer model very well (right).

© 2016 SEG

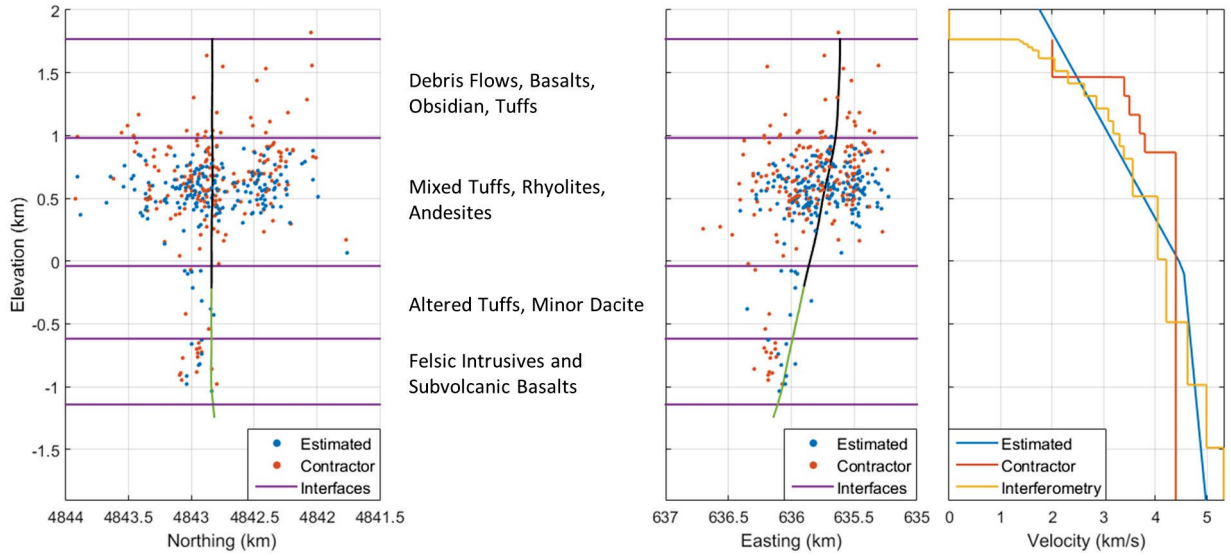

Figure 3: Comparison between our simultaneous location result and that provided by the contractor. The simultaneous location result is more clustered than the contractor's result. It is well confined below the units interface at the elevation around 1.0 km. The simultaneously inverted velocity model is very close to that obtained by seismic interferometry compared with the contractor's model.

space**EDITED REFERENCES**

Note: This reference list is a copyedited version of the reference list submitted by the author. Reference lists for the 2016 SEG Technical Program Expanded Abstracts have been copyedited so that references provided with the online metadata for each paper will achieve a high degree of linking to cited sources that appear on the Web.

REFERENCES

Aki, K., and P. Richards, 1980, Quantitative seismology: Theory and methods: WH Freeman & Co.

Cladouhos, T. T., S. Petty, Y. Nordin, M. Moore, K. Grasso, M. Uddenberg, M. Swyer, B. Julian, and G. Foulger, 2013, Microseismic monitoring of newberry volcano egs demonstration: Proceedings of the 38th Workshop on Geothermal Reservoir Engineering, 11–13.

Douglas, A., 1967, Joint epicentre determination: Nature, **215**, 47–48, http://dx.doi.org/10.1038/215047a0.

Drew, J. E., H. D. Leslie, P. N. Armstrong, and G. Michard, 2005, Automated microseismic event detection and location by continuous spatial mapping: Presented at the SPE Annual Technical Conference and Exhibition, SPE.

Duncan Peter, M., and L. Eisner, 2010, Reservoir characterization using surface microseismic monitoring: Geophysics, **75**, 139–146, http://dx.doi.org/10.1190/1.3467760.

Eisner, L., P. M. Duncan, W. M. Heigl, and W. R. Keller, 2009, Uncertainties in passive seismic monitoring: The Leading Edge, 28, 648–655.

Hayles, K., R. L. Horine, S. Checkles, J. Blangy, 2011, Comparison of microseismic results from the bakken formation processed by three different companies: Integration with surface seismic and pumping data: Presented at the 81st Annual International Meeting, SEG, Expanded Abstracts, http://dx.doi.org/10.1190/1.3627479.

Li, J., H. Zhang, W. L. Rodi, and M. N. Toksoz, 2013, Joint microseismic location and anisotropic tomography using differential arrival times and differential backazimuths: Geophysical Journal International, 195, 1917–1931, http://dx.doi.org/10.1093.gji/ggt358.

Matzel, E., D. Templeton, A. Petersson, and M. Goebel, 2014, Imaging the newberry egs site using seismic interferometry: Proceedings of the 39th Workshop on Geothermal Reservoir Engineering, 24–26.

Maxwell, S., 2009, Microseismic location uncertainty: CSEG Recorder.

Monteiller, V., J.-L. Got, J. Virieux, and P. Okubo, 2005, An efficient algorithm for double-difference tomography and location in heterogeneous media, with an application to the kilauea volcano: Journal of Geophysical Research: Solid Earth, **110**, http://dx.doi.org/10.1029/2004JB003466.

© 2016 SEG

Myers, S. C., G. Johannesson, andW. Hanley, 2007, A bayesian hierarchical method for multiple-event seismic location: Geophysical Journal International, 171, 1049–1063.
Myers, S. C., G. Johannesson, and W. Hanley, 2009, Incorporation of probabilistic seismic phase labels into a bayesian multiple-event seismic locator: Geophysical Journal International, **177**, 193–204, http://dx.doi.org/10.1111/j.1365-246X.2008.04070.x.
Oliver, D. S., A. C. Reynolds, and N. Liu, 2008, Inverse theory for petroleum reservoir characterization and history matching: Cambridge University Press.
Osborn, W., S. Petty, L. Nofziger, and D. Perry, 2010, Newberry volcano egs demonstration: GRC Transactions, **34**, 1213–1220.
Osborn,W. L., S. Petty, T. T. Cladouhos, J. Iovenitti, L. Nofziger, O. Callahan, D. S. Perry, and P. L. Stern, 2011, Newberry volcano egs demonstration-phase i results: Technical report, AltaRock Energy Inc.
Petty, S., Y. Nordin, W. Glassley, T. T. Cladouhos, and M. Swyer, 2013, Improving geothermal project economics with multi-zone stimulation: results from the newberry volcano egs demonstration: Proceedings of the 38th Workshop on Geothermal Reservoir Engineering, 11–13.
spacePoliannikov, O. V., M. Prange, A. E. Malcolm, and H. Djikpesse, 2014, Joint location of microseismic events in the presence of velocity uncertainty: Geophysics, **79**, KS51–KS60, http://dx.doi.org/10.1190/geo2013-0390.1.
Slawinski, R. A., and M. A. Slawinski, 1999, On raytracing in constant velocity-gradient media: Calculus approach: Canadian Journal of Exploration Geophysics, **35**, 24–27.
Tarantola, A., 2005, Inverse problem theory and methods for model parameter estimation: SIAM.
Tarantola, A., and B. Valette, 1982, Inverse problems = quest for information: Journal of Geophysics, **50**, 150–170.
Templeton, D. C., G. Johannesson, and S. C. Myers, 2014, An investigation of the microseismicity at the newberry egs site: Technical report, Lawrence Livermore National Laboratory (LLNL).
Waldhauser, F., and W. L. Ellsworth, 2000, A double-difference earthquake location algorithm: Method and application to the northern hayward fault, california: Bulletin of the Seismological Society of America, **90**, 1353–1368, http://dx.doi.org/10.1785/0120000006.
Warpinski, N., 2009, Microseismic monitoring: Inside and out: Journal of Petroleum Technology, **61**, 80–85, http://dx.doi.org/10.2118/118537-MS.
Zhang, H., S. Sarkar, M. N. Toksöz, H. S. Kuleli, and F. Al-Kindy, 2009, Passive seismic tomography using induced seismicity at a petroleum field in oman: Geophysics, **74**, WCB57–WCB69, http://dx.doi.org/10.1190/1.3253059.
Zhang, H., and C. H. Thurber, 2003, Double-difference tomography: The method and its application to the Hayward fault, California: Bulletin of the Seismological Society of America, **93**, 1875–1889, http://dx.doi.org/10.1785/0120020190.
Zhang, Z., B. Jafarpour, and L. Li, 2014, Inference of permeability heterogeneity from joint inversion of transient flow and temperature data: Water Resources Research, **50**, 4710–4725, http://dx.doi.org/10.1002/2013WR013801.
Zhang, Z., J. W. Rector, and M. J. Nava, 2015a, Microseismic event location using multiple arrivals: Demonstration of uncertainty reduction: Presented at the Unconventional Resources Technology Conference (URTEC), http://dx.doi.org/10.15530/urtec-2015-2153641.
Zhang, Z., J. W. Rector, M. J. Nava, 2015b, Improving microseismic event location accuracy with head wave arrival time: Case study using marcellus shale: Presented at the 85th SEG Annual International Meeting, SEG, Expanded Abstracts, http://dx.doi.org/10.1190/segam2015-5919420.1.
Zhou, R., L. Huang, and J. Rutledge, 2010, Microseismic event location for monitoring co2 injection using double-difference tomography: The Leading Edge, **29**, 208–214, http://dx.doi.org/10.1190/1.3304826

© 2016 SEG

tional probability density of data $\mathbf{d}$ given model parameters $\mathbf{m}$, and $\mu_D(\mathbf{d})$ is the homogeneous probability density in data space.

The marginal probability density of model parameters $\mathbf{m}$ is the integration of the joint probability density over the entire data space $\mathfrak{D}$:

$$\sigma_M(\mathbf{m}) = \int_{\mathfrak{D}} d\mathbf{d}\, \sigma(\mathbf{d},\mathbf{m}). \quad (2)$$

If the model and data space of the system are both linear, under Gaussian assumption, the posterior probability density of the model parameters can be expressed by

$$\sigma_M(\mathbf{m}) = c\exp[-O(\mathbf{m})], \quad (3)$$

and

$$O(\mathbf{m}) = \frac{1}{2}[\mathbf{g}(\mathbf{m}) - \mathbf{d}_{obs}]^T \mathbf{C}_D^{-1}[\mathbf{g}(\mathbf{m}) - \mathbf{d}_{obs}] + \frac{1}{2}(\mathbf{m} - \mathbf{m}_{prior})^T \mathbf{C}_M^{-1}(\mathbf{m} - \mathbf{m}_{prior}), \quad (4)$$

yet important characterization of the conditional parameter distribution.

The above minimization can be implemented using the classical Gauss-Newton method. Once the MAP estimate $\mathbf{m}_{MAP}$ is found, the posterior covariance matrix $\mathbf{C}_{m,MAP}$ can be approximated through linearization about the MAP estimate as

$$\mathbf{C}_{m,MAP} = \mathbf{C}_M - \mathbf{C}_M \mathbf{G}_{MAP}^T \left(\mathbf{G}_{MAP}\mathbf{C}_m \mathbf{G}_{MAP}^T + \mathbf{C}_D\right)^{-1} \mathbf{G}_{MAP}\mathbf{C}_M, \quad (6)$$

where, $\mathbf{G}_{MAP}$ is the sensitivity matrix at the MAP point with elements $G_{ij} = \frac{\partial g_i}{\partial m_j}$.

© 2016 SEG